Small angle neutron scattering

Focus on magnetic nanoparticles and biological applications

A.V.Belushkin

Frank Laboratory of Neutron Physics, JINR, Dubna, Russia

Small Angle Neutron Scattering (SANS)

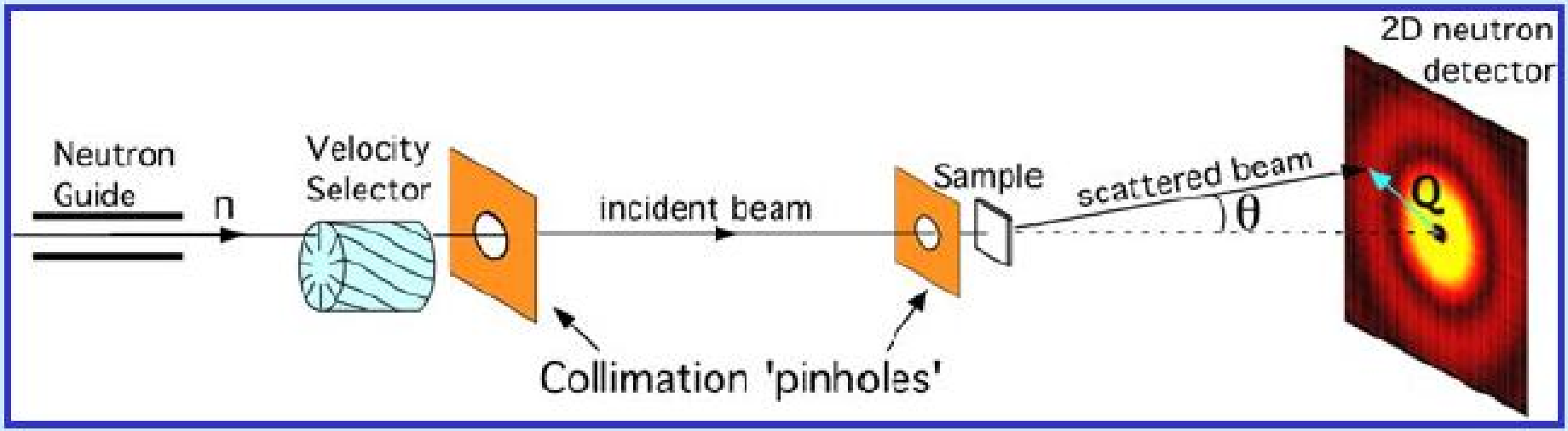

Small-Angle Neutron Scattering (SANS) probes structure on a scale d, where

$$d \approx \frac{\lambda}{\theta}$$ (wavelength) / (scattering angle)

$0.5 \text{ nm} < \lambda < 2 \text{ nm}$ (cold neutrons)

$0.1^\circ < \theta < 10^\circ$ (small angles)

$1 \text{ nm} < d < 300 \text{ nm}$

Examples of registered patterns on a detector

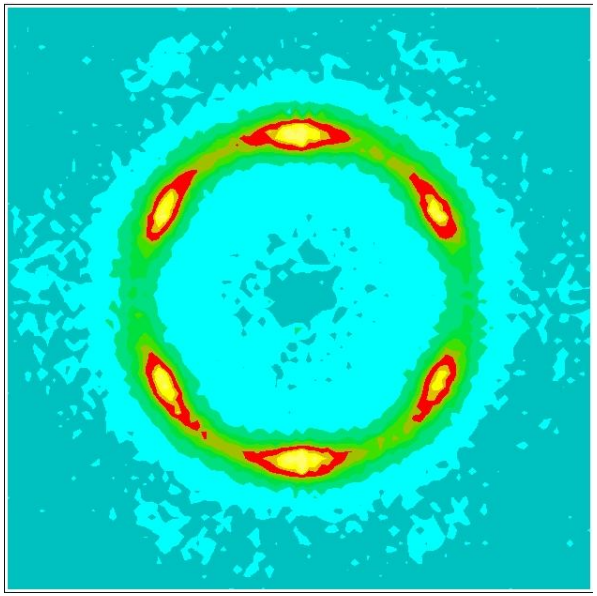

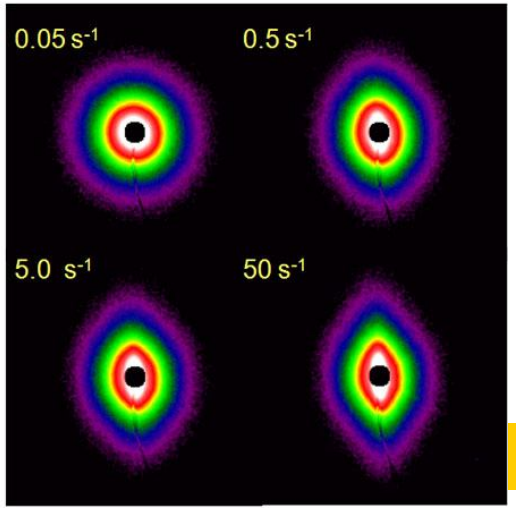

From the analysis of the signal on a detector, using advanced mathematical models one can extract information about characteristic sizes, shape and relative orientation as well as some other parameters of the nanoparticles in a sample under investigation

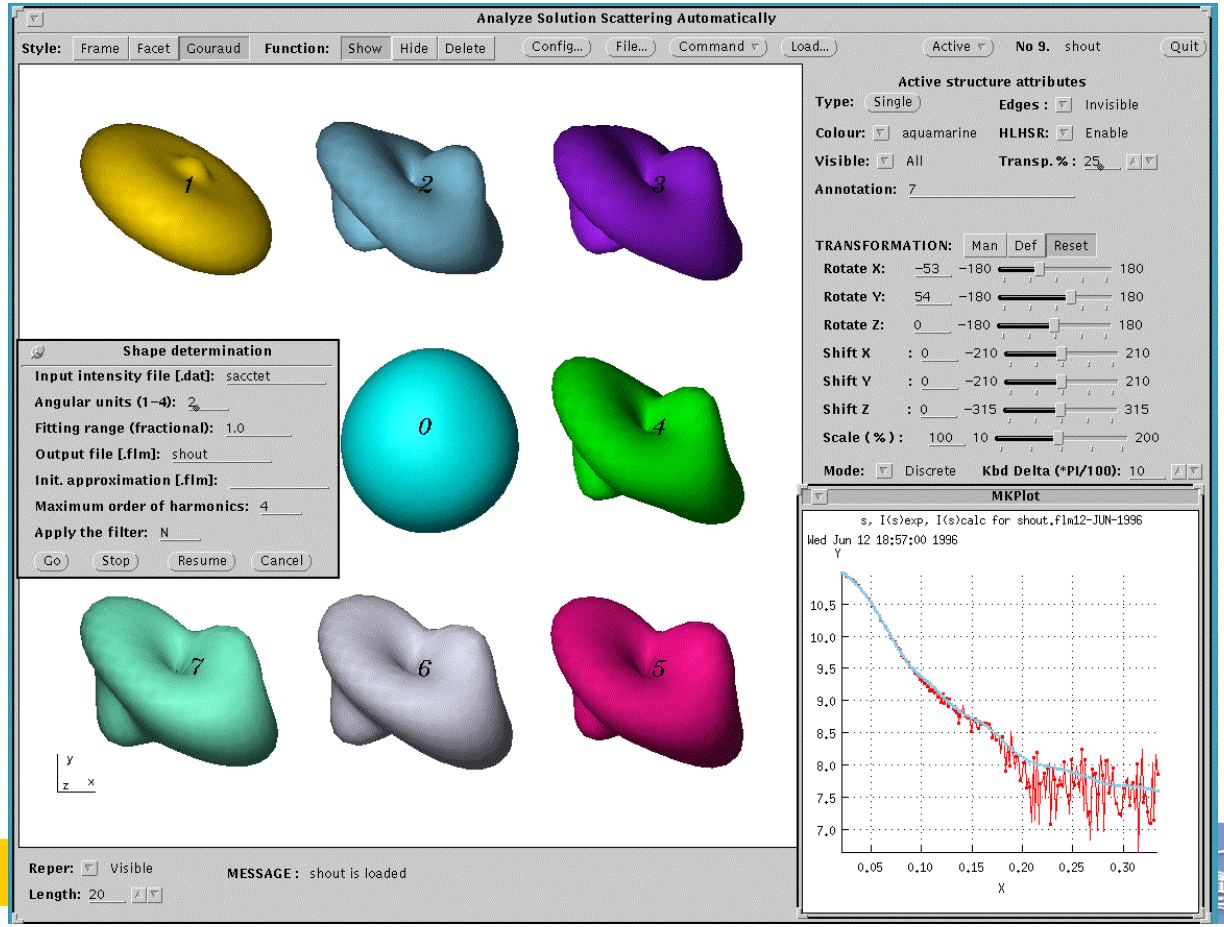

SANS applicability

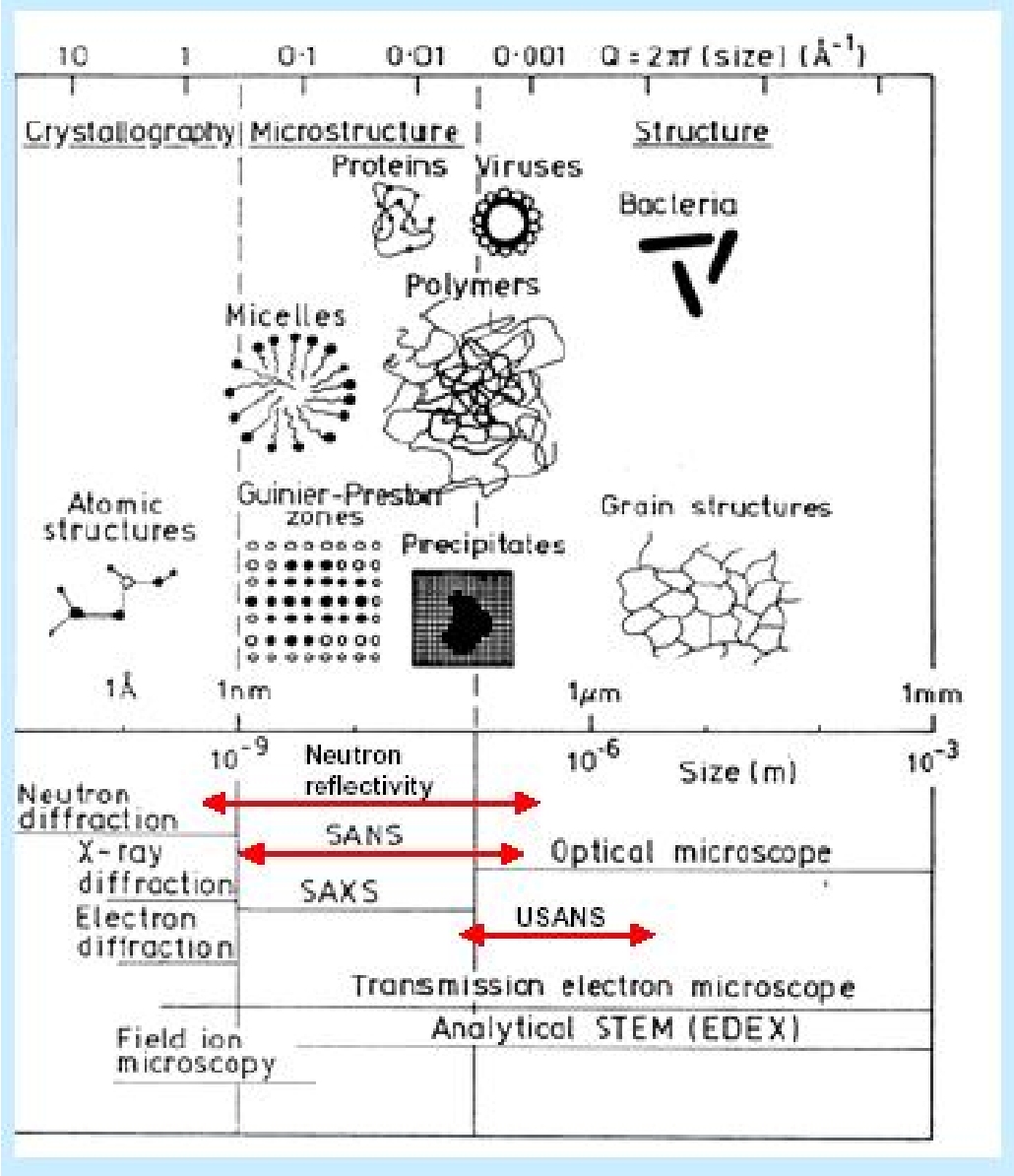

Основные теоретические представления

При рассмотрении малоуглового рассеяния нейтронов вводится понятие пространственного распределения плотности когерентной амплитуды рассеяния

$$\rho\ (\vec{r}) = \bar{b} \times N_a(\vec{r})$$

где *b* - средняя когерентная амплитуда рассеяния нейтронов для частицы (или соответственно растворителя), N_a - распределение атомной плотности в частице (или растворителе), имеющее размерность [число атомов / единица объема]. Потенциал взаимодействия нейтрона с таким объектом может быть записан в виде

$$H_c = \frac{2\ \pi\ \hbar^2}{m} \rho\ (\vec{r})$$

При рассеянии плоской нейтронной волны на таком потенциале амплитуда упругого и когерентного рассеяния будет пропорциональна матричному элементу

$$\left\langle \vec{k}_1 \middle| H_c \middle| \vec{k}_0 \right\rangle$$

$$\left\langle \vec{k}_1 \middle| H_c \middle| \vec{k}_0 \right\rangle = A(\vec{Q}) = \int_V \rho(\vec{r}) exp(i\vec{Q}\vec{r}) d\vec{r}$$

где интегрирование идет по всему объему исследуемого образца. Интенсивность рассеянной волны пропорциональна дифференциальному сечению рассеяния, т.е. квадрату матричного элемента.

$$I(\vec{Q}) \sim \frac{d\sigma}{d\Omega} = \left| A(\vec{Q}) \right|^2 = \left| \int_V \rho(\vec{r}) exp(i\vec{Q}\vec{r}) d\vec{r} \right|^2$$

Задача исследования методом малоуглового рассеяния состоит в восстановлении функции ***ρ(r)*** в исследуемом объекте по измеренной зависимости ***I(Q)***. Степень разрешимости этой задачи зависит от многих факторов. Рассмотрим некоторые наиболее часто используемые приближения.

$\vec{Q}$

Изотропное распределение частиц в растворе

Выражение для сечения рассеяния следует усреднить по всем возможным пространственным ориентациям частиц относительно вектора рассеяния:

$$\left\langle \frac{d\,\sigma}{d\,\Omega} \right\rangle = \int_{V}\int_{V'} \rho\,(\vec{r})\,\rho\,(\vec{r}\,')\,\frac{sinQ|\vec{r}\,-\vec{r}\,'|}{Q|\vec{r}\,-\vec{r}\,'|}\,d\,\vec{r}\,\,d\,\vec{r}\,'$$

Формула носит название формулы Дебая. Она получается на основе следующих соотношений

$$\left\langle \sin[\vec{Q}(\vec{r}-\vec{r}\,')] \right\rangle = \int_{0}^{\pi} \sin(Q|\vec{r}-\vec{r}\,'|\cos\varphi\,)\,\frac{\sin\,\varphi}{2}\,d\varphi\,=0$$

$$\left\langle \cos[\vec{Q}(\vec{r}-\vec{r}\,')] \right\rangle = \int_{0}^{\pi} \cos(Q|\vec{r}-\vec{r}\,'|\cos\varphi\,)\,\frac{\sin\varphi}{2}\,d\varphi\,=\frac{\sin Q|\vec{r}-\vec{r}\,'|}{Q|\vec{r}-\vec{r}\,'|}$$

Здесь φ - угол между векторами Q и r-r' , а $sin(\varphi)d\varphi/2$ - вероятность того, что угол φ заключен в интервале от φ до $\varphi + d\varphi$.

Во всех вышеприведенных рассуждениях мы считали, что частицы находятся в вакууме, т.е. не учитывали свойств растворителя. Все вышеприведенные формулы при учете растворителя остаются справедливыми, если заменить ρ на ρ - ρ_s , где ρ_s - плотность когерентного рассеяния растворителя. При этом вводится важное понятие **контраста**.

Контраст – разницы между средней плотностью рассеяния частицы и плотностью рассеяния растворителя:

$$\Delta\rho = \left\langle \rho(\vec{r}) - \rho_s \right\rangle = \frac{1}{V} \int_V \left[\rho(\vec{r}) - \rho_s \right] d\vec{r} = \bar{\rho} - \rho_s$$

При больших значениях $\Delta\rho$ (сильный контраст) сигнал от частиц будет велик по сравнению с сигналом от растворителя, т.е. частицы будут ясно "видны" в малоугловом рассеянии. Наоборот, при слабом контрасте сигнал от частиц будет практически неотделим от общего сигнала. Поэтому контраст является одной из важнейших характеристик в малоугловых экспериментах. **Вариация контраста**, т.е. изменение значения $\Delta\rho$, например, за счет изотопного замещения служит мощным инструментом получения дополнительной структурной информации.

Схематическая иллюстрация вариации контраста

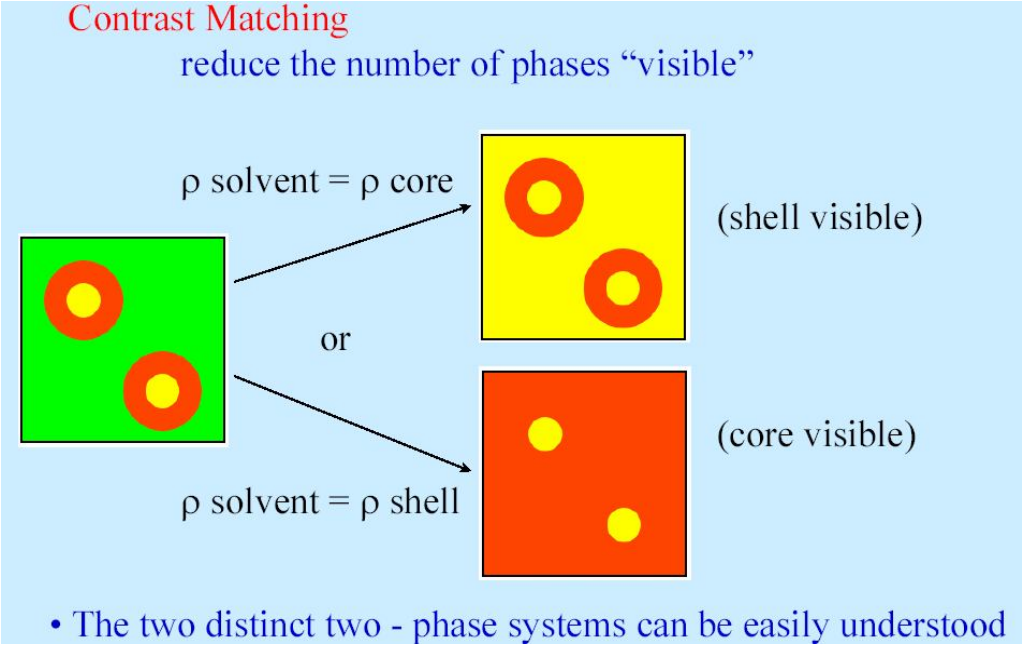

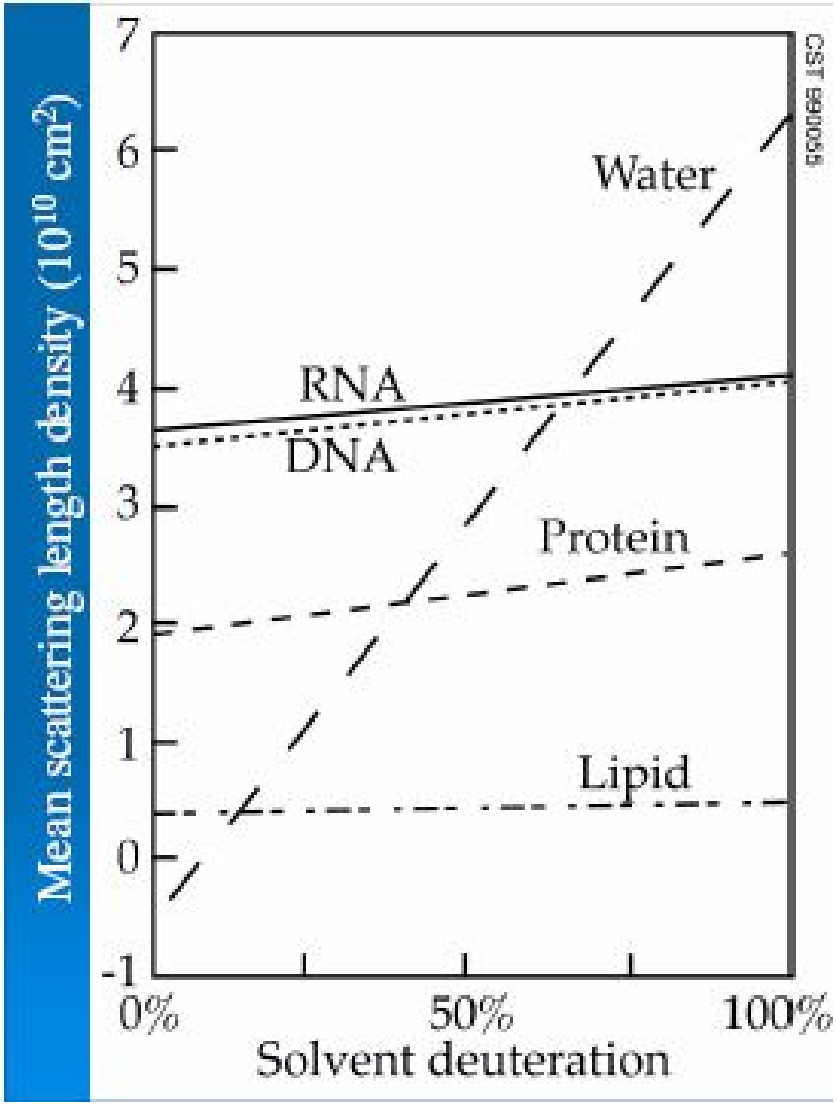

Guinier approximation

in 1939 A.Guinier simplified Debye formula for $QL<<1$. using an expansion $\sin x/x = 1 - x2/3! + x4/5! - \ldots$ And keeping only the first two terms, Debye formula becomes

$$I(Q) \sim \left\langle \frac{d\sigma}{d\Omega} \right\rangle = \left(\int_V \rho(\vec{r}) d\vec{r} \right)^2 \left(1 - \frac{1}{3} Q^2 \int_V \rho(\vec{r}) r^2 d\vec{r} \Big/ \int_V \rho(\vec{r}) d\vec{r} + \ldots \right) =$$

$$= \left(\int_V \rho(\vec{r}) d\vec{r} \right)^2 \left((1 - Q^2 R^2{}_g / 3 + \ldots \right),$$

where R^2_g is the radius of gyration with the replacement of the body mass density for scattering density.

Guinier assumed that the expression in last parenthesis can be written in a form

$$F^2(Q) = \exp(-Q^2 R_g^2 / 3)$$

This expression is the basis for extracting the particle radius of gyration from the experimental data. For this purpose the data are plotted as the so called Guinier plot - ***lnI*(Q^2)** and inclination angle gives us R_g:

$$R_g^2 = -\frac{1}{3} d\ \mathrm{lnI}(Q^2) / dQ^2$$

Forward scattering

For $Q = 0$ the differential cross section becomes

$$\left\langle \frac{d\sigma}{d\Omega} \right\rangle = (\bar{\rho} - \rho_s)^2 V^2$$

By using $I(0)$ one can estimate both particle volume and its molecular mass. For molecular mass estimation one needs the knowledge of average coherent scattering length density and an independently measured a partial specific particle volume

$$\bar{v} = \frac{VN_A}{M}$$

where N_A – is the Avogadro number. Then one has

$$I(0) = N\left\langle \frac{d\sigma}{d\Omega} \right\rangle = N(\bar{\rho} - \rho_s)^2 V^2 = Mc(\bar{\rho} - \rho_s)^2 \bar{v}^2 V_s \cdot N_A^{-1}$$

where N – is the total number of particles in solution, which can be calculated from their weight concentration C (g mole/l) $(M \cdot N)/(V_s/N_A)$, V_s – solvent volume.

Porod integral

One of the important integral characteristic of SANS is the so-called Porod invariant

$$A = \int_0^\infty Q^2 I(Q) dQ = 2\pi^2 \int_V [\rho(\vec{r}) - \rho_s]^2 d\vec{r}$$

Porod invariant characterizes the total scattering power of the object under investigation and is proportional to the square of the particle contrast with respect of the solvent. It is used for calculations of different structural parameters. In the case of uniform density particle, Porod invariant directly gives us a particle volume

$$A = 2\pi^2 (\overline{\rho} - \rho_s)^2 \cdot V$$

In the limit $Q \to \infty$ for the uniform density particles one gets

$$I(Q) \underset{Q\to\infty}{=} \frac{2\pi}{Q^4}(\bar{\rho} - \rho_s)^2 S$$

where S – is the surface area of a particle. Therefore, for the uniform particles it is possible to extract information about their surface area

Information which can be extracted from different parts of the SANS curve

Small Angle Neutron Scattering (SANS) from magnetic nanoparticles in solution

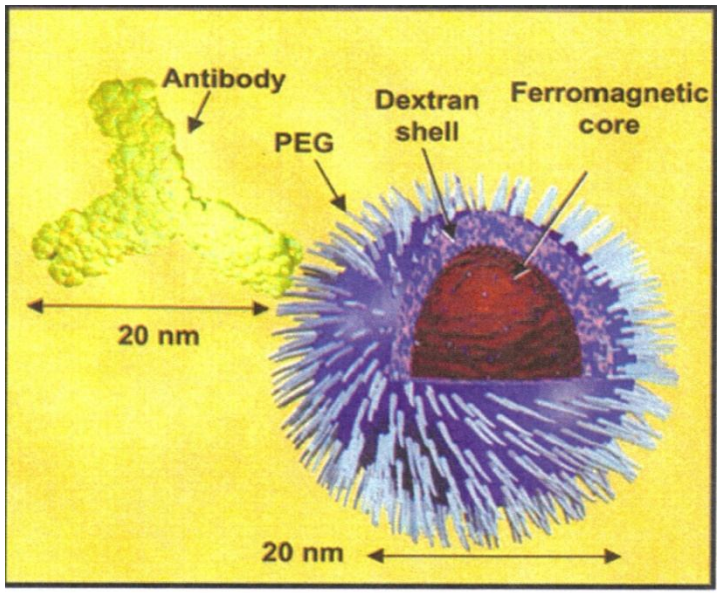

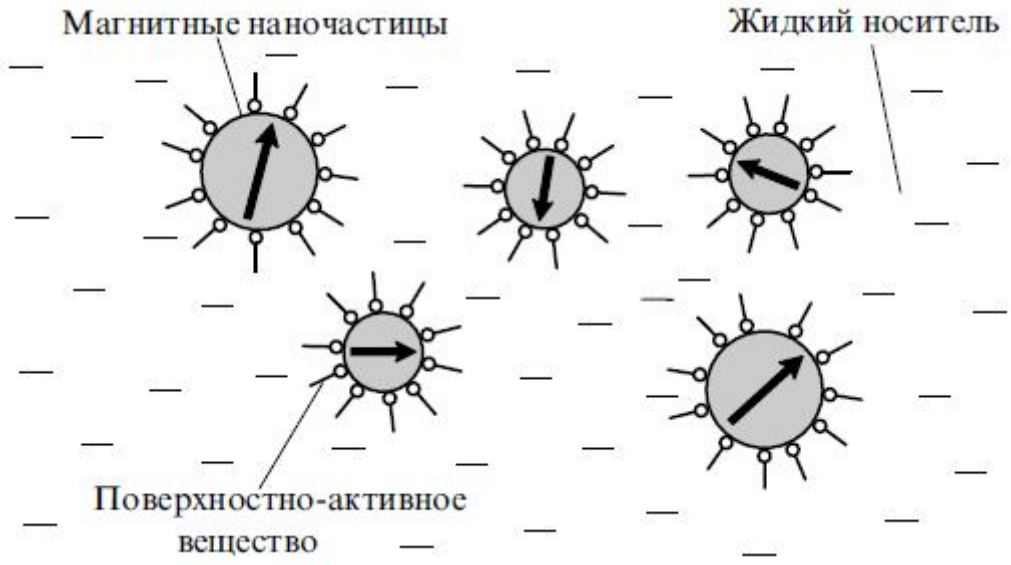

Scattering from a single nanoparticle:

- Nuclear scattering from magnetic core
- Nuclear scattering from hydrogen containing shell
- Magnetic scattering from magnetic core
- Nuclear scattering from the solvent

SANS from magnetic nanoparticles in solution

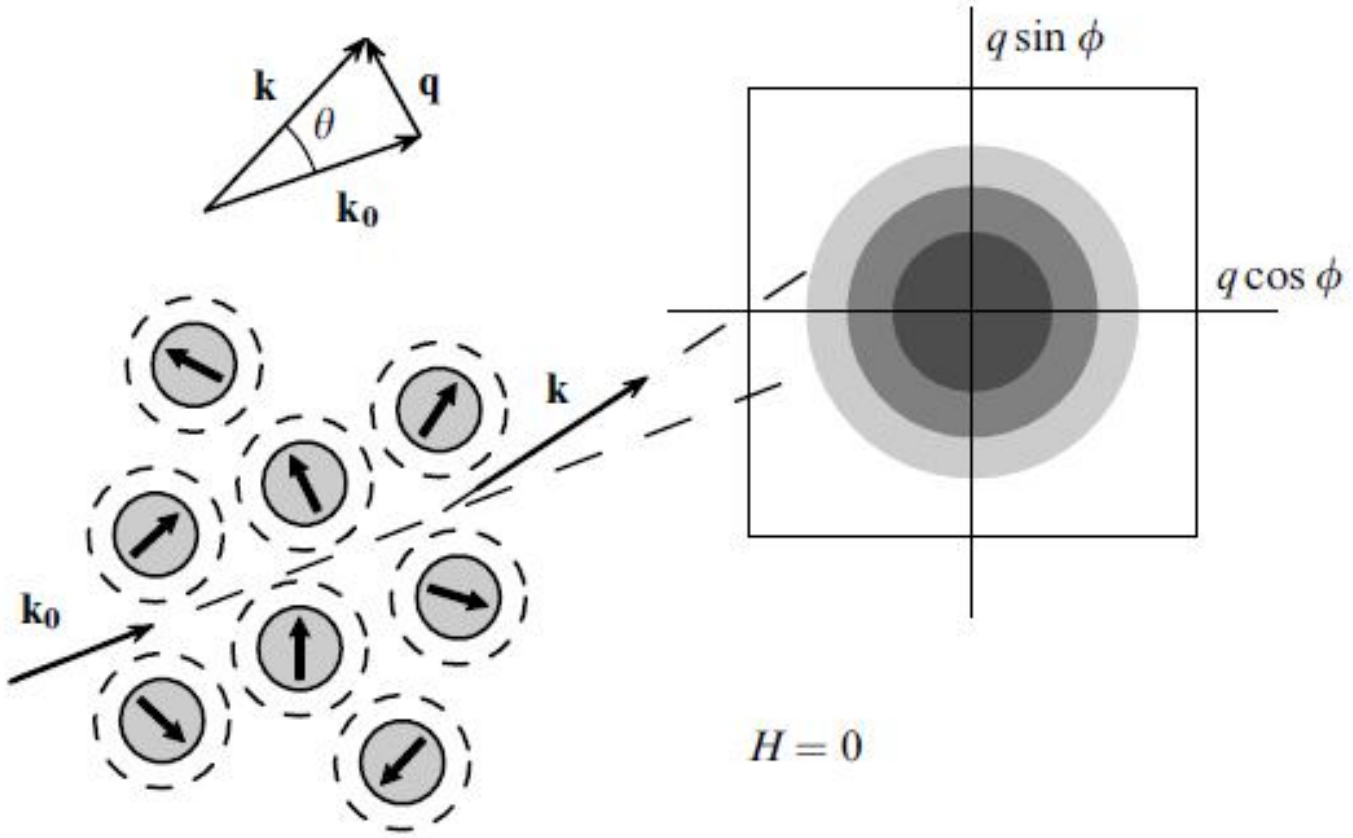

Principal scheme of SANS on magnetic nanoparticles in solution. In the absence of external magnetic field magnetic moments of nanoparticles are randomly oriented in space.

SANS from magnetic nanoparticles in solution

To separate magnetic and nuclear scattering one can use an external magnetic field. In general, nuclear scattering will not depend on the magnetic field (assuming that particles are almost spherical in shape) and magnetic scattering will be strongly field dependent. This follows from the expressions for the corresponding differential cross-sections.

$$\left\langle \frac{d\sigma}{d\Omega} \right\rangle_{nuclear} = (\overline{\rho} - \rho_s)^2 V^2 F^2(Q)$$

$$\frac{d\sigma}{d\Omega}_{magnetic} = const \cdot M^2 V^2 F^2(Q) sin^2(\Phi)$$

Where *V* – particle volume, *F(Q)* – particle form factor, *M* – particle magnetic moment, Φ - is an angle between particle magnetic moment and the neutron scattering vector *Q* (in practice, this is the azimuthal angle on the two-dimensional SANS detector).

SANS from magnetic nanoparticles in solution

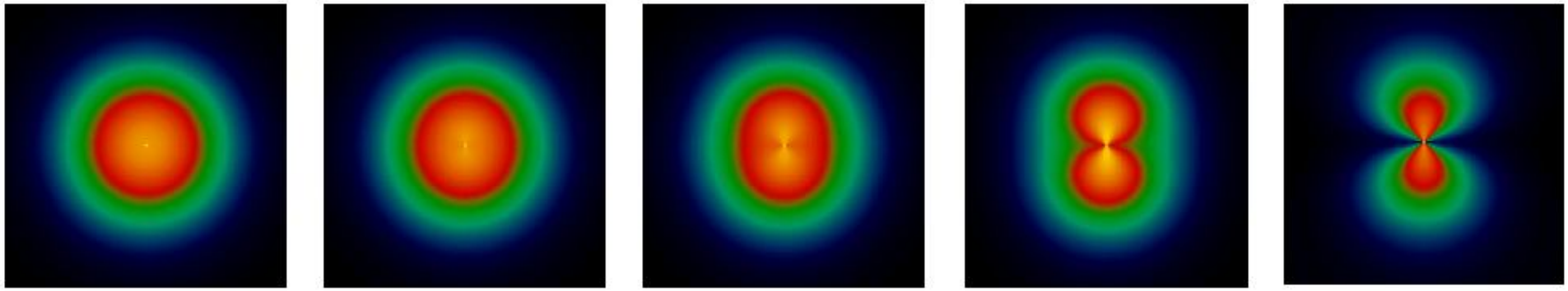

Simulated 2-dimensional magnetic SANS patterns of superparamagnetic particles in a nonmagnetic matrix. The transition from fully random magnetic orientation of the particles (left figure) to a strong field-parallel alignment (the very right figure) is clearly observed (the hypothetic field is directing horizontally).

SANS from magnetic nanoparticles in solution

Once the magnetic contribution is separated, then by using the contrast variation method it is possible to measure the nuclear radius of the magnetic core as well as the thickness of the polymeric shell.

Obviously we have considered a very simplified situation.

In reality the polydispersity of the particles size, non-spherical shape of the particles, effect of interaction between particles and the very nature of the colloidal systems (which magnetic nanoparticles in solution belong to) being intrinsically non-equilibrium, complicates the data analysis to great extent.

SANS from magnetic nanoparticles in solution

However, it was possible to extract many important characteristics (see e.g. Physics-Uspekhi, 53, 971-993, 2010) like

- **Nuclear radius of the magnetic core and thickness of the shell**
- **Size distribution of the nanoparticles**
- **Difference between nuclear and magnetic radii of the core**
- **Temperature behavior of the particles cluster sizes**
- **Comparison of interparticle interaction for different systems**
- **etc.**

SANS investigations of structural changes in living mitochondria

Inner mitochondrial membrane-

location of energy generating system of mitochondrion

SANS investigations of structural changes in living mitochondria

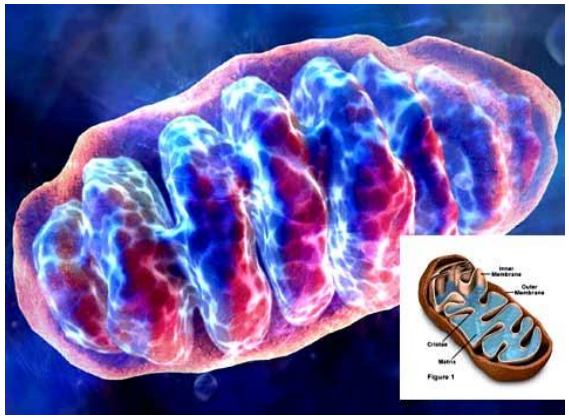

Isotonic
Normal condition

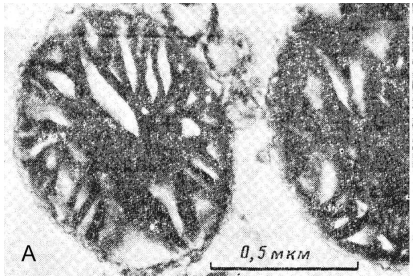

Formation of **"dried crista"**
Changes in function

Hypotonic
Low-amplitude swelling

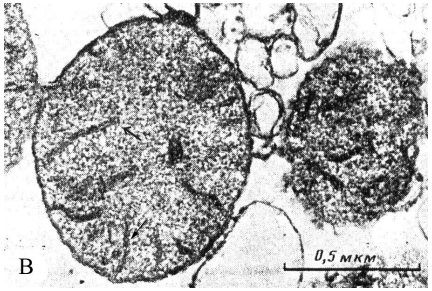

Hypotonic media induces changes in mitochondrial function:

- regulates the oxidation of fatty acid and other substrates.
- induces the rising of rate of the electron transport through the respiratory chain
- rising of rate and efficiency of ATP sythesis
- structural changes in polyenzymatic complex of oxidative phosphorilation
- switching on the local coupling regime
- imitation of hormone effect on mitochondria.

Different packing of inner mitochondrial membranes

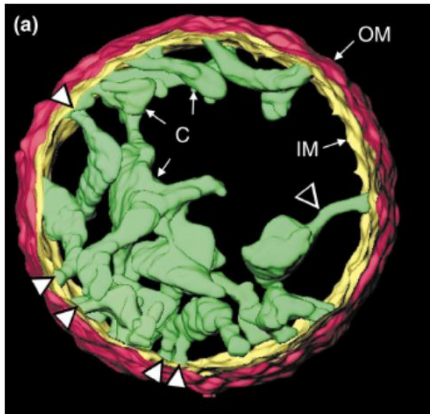

Томография митохондрий **печени** крысы

T.G. Frey, TIBS V.25, 2000, p. 319-324

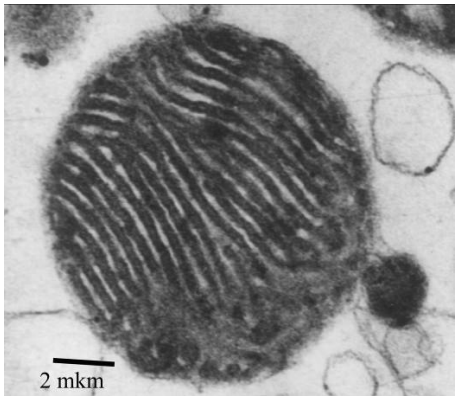

Митохондрии **сердца** крысы

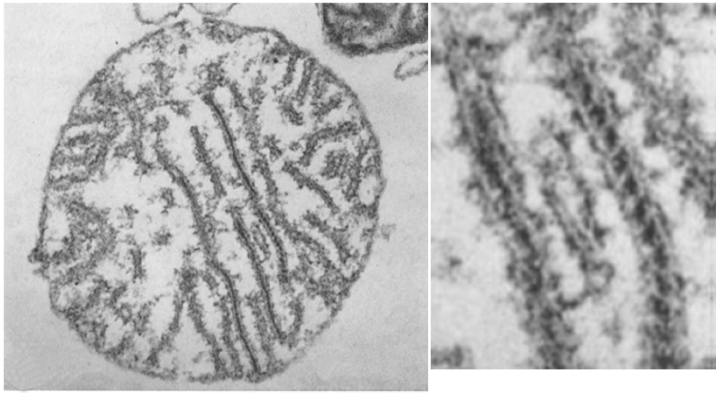

Предшественники гексагональной фазы

Митохондрии сердца быка

J. Hall and F. Crane, The J. Cell Biology, V.48, 1971, p. 420-425

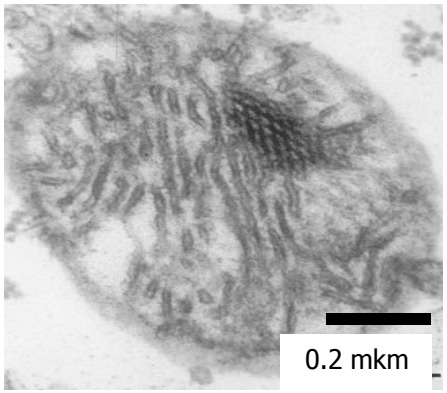

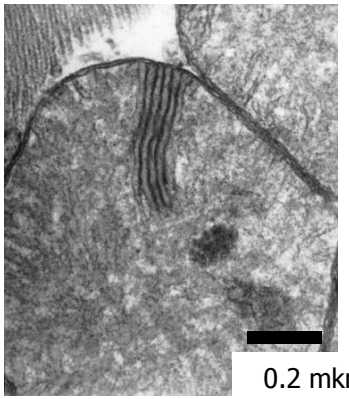

Гексагональная фаза

Митохондрии сердца крысы при апоптозе

Сапрунова В.Б., Бакеева Л.Е., Ягужинский Л.С. // Цитология. 2003. Т. 45. С. 1073-1082

Кубическая фаза

Митохондрии голодающей амебы *C.Carolinensis.*

Оксидативный спесс

Y.Deng et al, Protoplasma (2002) 219: 160–167

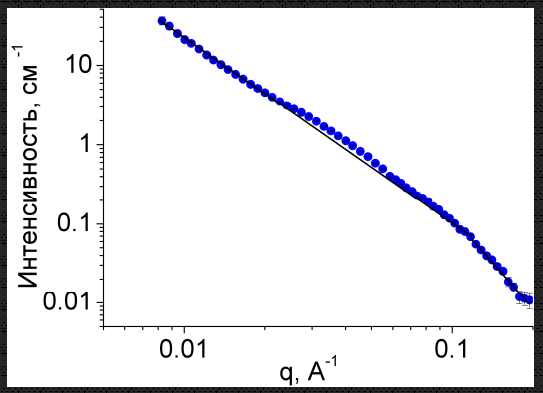

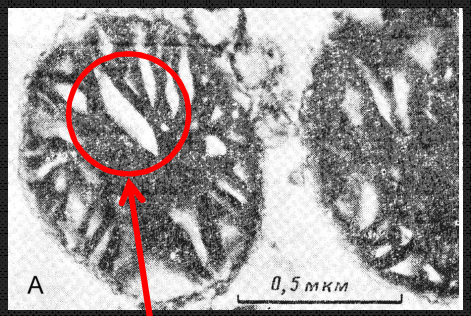

Expanded disordered cristae

No peaks

Krasinskaya I. et al. // *Biokhimija* 1989, V. 54: 1550-1556.
Murugova T. et al. // Biophysics 2006, V.51: 882-886.

Hypotonic conditions

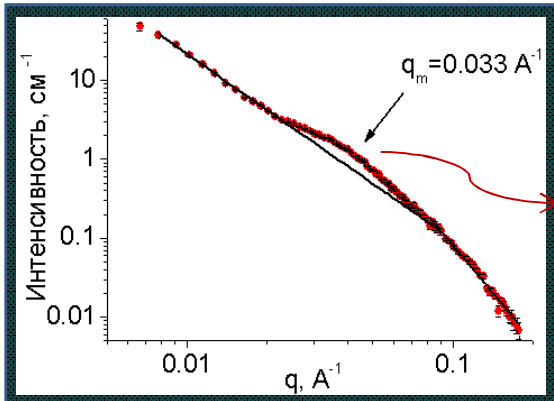

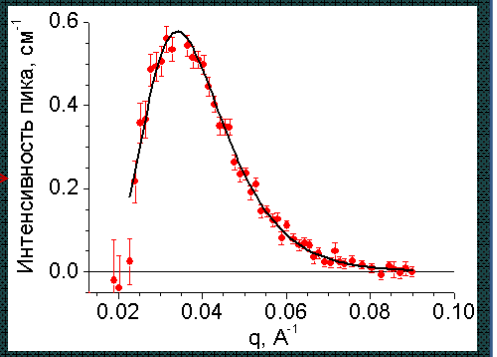

Extracted interference peak

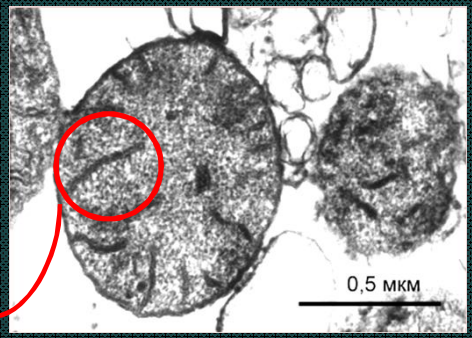

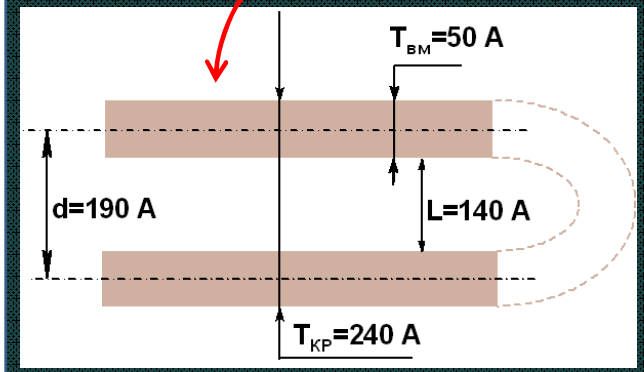

Scheme of ***dried ordered cristae*** formed under hypotonic conditions

Comparison of double membrane structural parameters obtained by different methods.

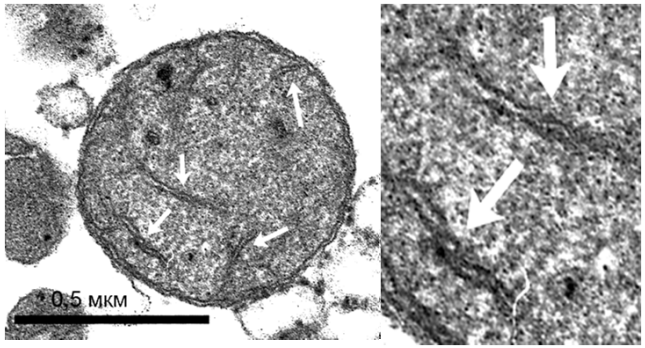

Hypotonic medium

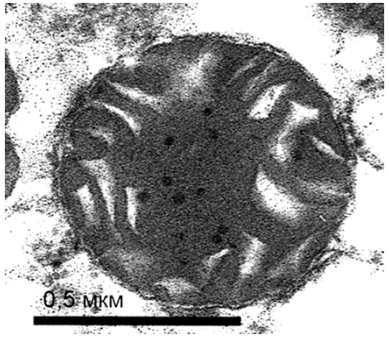

Isotonic medium

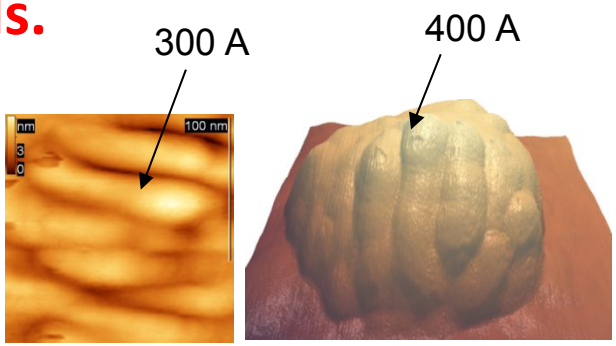

AFM data

Electron microscopy

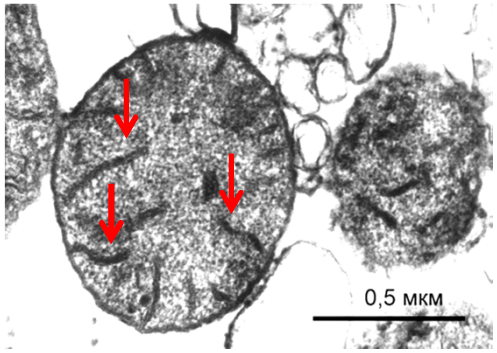

Красинская И.П., Литвинов И.С., Захаров С.Д., Бакеева Л.Е., Ягужинский Л.С. (1989), *Биохимия, 54(9), 1550-1556.*

Method	Double membrane structure thickness, Å
SANS (alive, statistical average)	240±10 *265±10
Electron microscopy (dead, individual)	220±20 #250±30
AFM (dead, individual)	300-400

* С учетом литературных данных о толщине внутренней митохондриальной мембраны
# Фотография из работы Красинская И.П., Литвинов И.С., Захаров С.Д., Бакеева Л.Е., Ягужинский Л.С. (1989), *Биохимия, 54(9), 1550-1556.*
Dubrovin E.V., Murugova T.N., Motovilov K.A., Yaguzhinskii L.S., Yaminskii I.V. *Nanotechnologies in Russia* 2009;4:876–880.

Observation of asymmetric distribution of proteins with respect to the lipid membranes using contrast variation technique.

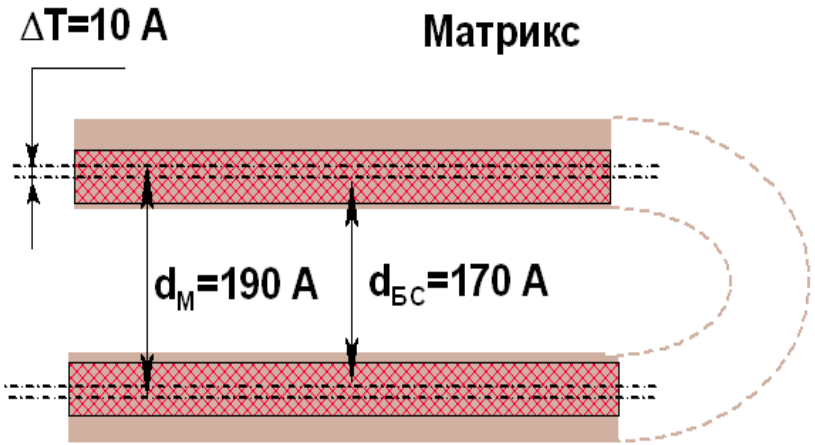

липидно-белковая мембрана, наблюдаемая в эксперименте с митохондриями в D_2O -среде

липидный бислой, наблюдаемый в эксперименте с митохондриями в 42%D_2O -среде

Distance between centres of double layer lipid membranes $d_{БС}$ =170Å

Distance between centres of double layer lipid membranes with imbedded proteins d_M =190 Å.

Centre of gravity for proteins is shifted towards matrix.

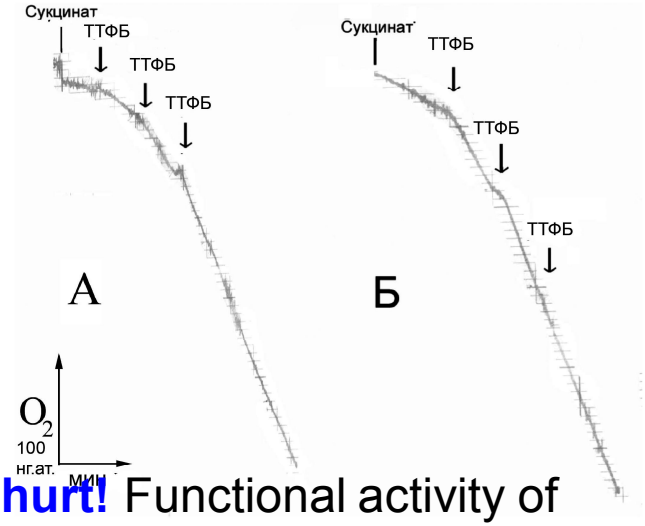

Neutrons do not hurt! Functional activity of mitochondria before (А) and after (Б) SANS experiment

Structure of the α-crystalline by small-angle neutron scattering (FLNP in collaboration with the Institute of biochemical physics RAN)

*A model of αB-crystallin with bound α-lactalbumin . **Electron microscopy**. Scale bar represents 100 Å.*
J. Horwitz, Exp. Eye Res. (2003) 76, 145-153

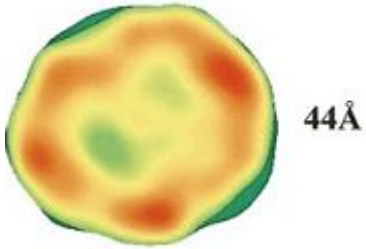

*Single particle reconstructions of native a-crystallin from **Electron microscopy**.*
D.A. Haley et al., J. Mol. Biol. (2000) 298, 261±272

- Oligomer protein (20-40 monomers, mass 400-1000 kDa)
- Polydisperse system
- Dinamical system (exchange of monomers)
- Difficult to crystallize

- This is the main component of the eye lens of vertebrae (200 mg/ml), which ensures a correct refractive index
- Exhibits chaperone like activity (forms soluble complexes with the destabilized proteins and prevents their non-specific aggregation and uncontrolled denaturation)
- Slows down the age related opacification of the eye lens (cataract)

Structure of the α-crystalline by small-angle neutron scattering (FLNP in collaboration with the Institute of biochemical physics RAN)

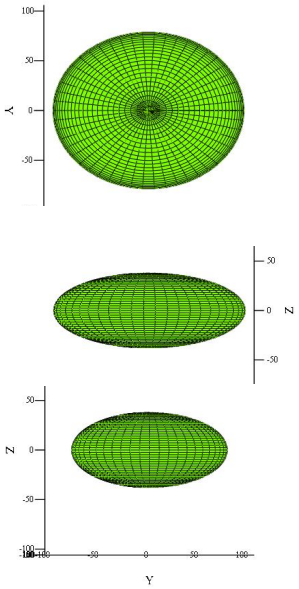

Approximation of the SANS data by the model of three-axis ellipsoid.

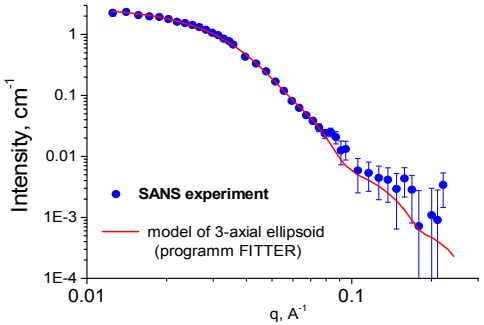

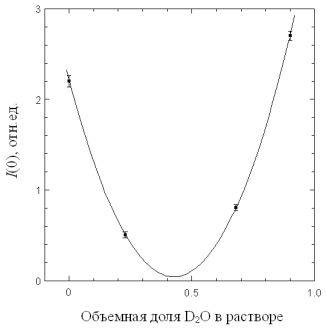

Experimental dependence of the scattering intensity at zero angle versus volume fraction of D_2O in the buffer solution and its approximation by parabolic function.

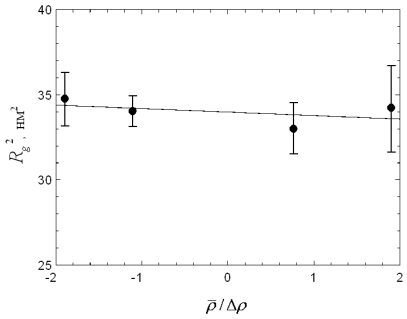

Experimental dependence of Vcrystalline radius of gyration versus contrast in buffer solution with different D_2O concentrations.

- **Uniform distribution of the scattering density in the protein parts inaccessible for water penetration.**
- **Absence of voids into which water cannot penetrate.**
- **All sub-units are equally accessible for water (perhaps for other low molecular weight substances, including bio active compounds).**

А. В. Кривандин, Т. Н. Муругова, А. И. Куклин, К. О. Муранов, Н. Б. Полянский, В. Л. Аксенов, М. А. Островский, Биохиммия **75** (11), 1499-1507 (2010).

Structure of the α-crystalline by small-angle neutron scattering (FLNP in collaboration with the Institute of biochemical physics RAN)

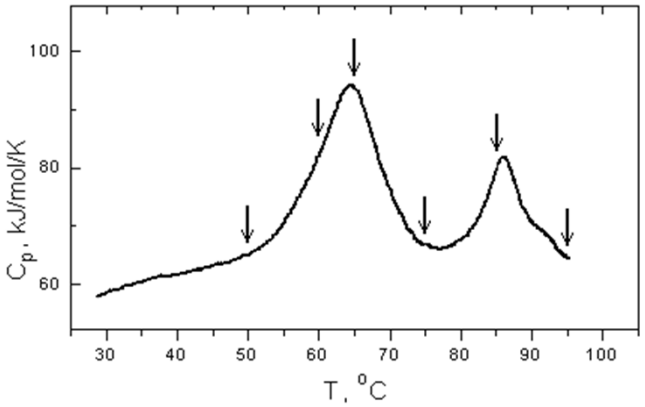

DSC data. Arrows indicate temperatures at which SANS data were measured.

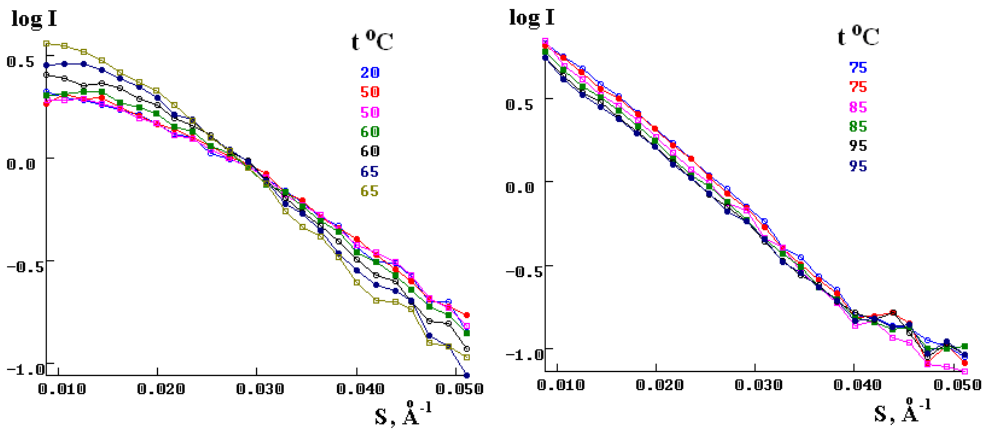

Changes of SANS curves for α crystalline in 90% D_2O-buffer during heating from 20 to 95°C.

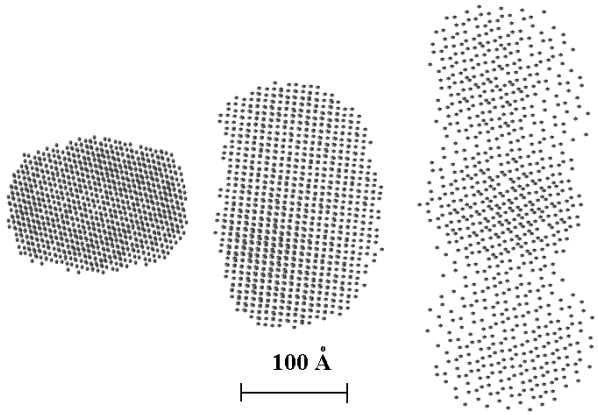

20 °C 65 °C 95 °C

- Protein dimerization at 60-65 °C
- Rod-like form at 75-95 °C

A. V. Krivandin, A. I. Kuklin, K. O. Muranov, **T. N. Murugova**, S. S. Kozlov, N. K. Genkina, "Heat-induced structural transitions of alpha-crystallin studied by small-angle neutron scattering", Journal of Physics: Conference Series, 2012, Vol. 351, 012008.

Complex study of nanostructures

- Electron microscopy
- Dynamic light scattering
- Static light scattering
- Quasi elastic neutron scattering
- X-ray and neutron diffraction
- X-ray and neutron reflectometry
- Small-angle X-ray and neutron scattering
- Sedimentation analysis
- Spectrometry
- Photometry
- Calorimetry ….